J Radioanal Nucl Chem (2016) 309:439–451
DOI 10.1007/s10967-016-4785-6

Trace and some rare earth elements distribution in a sediment profile from Jurumirim Reservoir, São Paulo State, Brazil: total content and extracted phases

R. L. Franklin[1] · S. A. Silva[1] · D. I. T. Fávaro[2] · W. Luiz-Silva[3]

Received: 1 October 2015 / Published online: 15 March 2016

Abstract Vertical distribution of some rare earth elements (REEs) and trace elements through a Jurumirim Reservoir sediment core is presented. REE fractionation using BCR sequential extraction protocol was performed to verify REE mobility in the environment. Three steps (exchangeable, reducible, oxidizable) and residual fractions were studied and REE distribution for each was evaluated by ICP-MS. REEs showed a higher affinity for the reducible phase. Instrumental neutron activation analysis was also applied to sediment samples to determine the total mass fraction for some REE (Ce, Eu, La, Lu, Nd, Sm, Tb, and Yb). The diagrams normalized to chondrite values were used for a REE distribution pattern evaluation.

Keywords REEs · Sediment profile · ICP-MS · ICP-OES · INAA · Sequential extraction protocol

✉ D. I. T. Fávaro
defavaro@ipen.br

R. L. Franklin
rfranklin@sp.gov.br; robleocadio@hotmail.com

W. Luiz-Silva
wanilson@ige.unicamp.br

[1] Laboratório de Química Inorgânica, Companhia Ambiental do Estado de São Paulo (CETESB), Av. Professor Frederico Hermann Jr. 345, São Paulo 05459-900, Brazil

[2] Laboratório de Análise por Ativação com Neutrons (LAN/CRPq), Instituto de Pesquisas Energéticas e Nucleares (IPEN – CNEN/SP), Av. Professor Lineu Prestes 2242, São Paulo 05508-000, Brazil

[3] Instituto de Geociências, UNICAMP, R. João Pandiá Calógeras 51, Campinas 13083-970, Brazil

Introduction

Reservoirs or dams are anthropogenic interventions in aqueous environments with the purpose of flood control, power generation or water collection for public consumption, among other functions [1]. This type of change in the water regime of the river causes substantial changes. When dammed, the speed of the water changes from the lotic regime, common to the river, to lentic regime, to a lower flow and speed. This reduction of flow rates facilitate the deposition of suspended particulate materials by water, accumulating these at the bottom of reservoirs, resulting in sedimentation.

The sediment is a compartment that has been increasingly used in studies of water quality ecosystem evaluation, by registering historical conditions of the anthropogenic activity influences on these environments, not always detectable by the use of variables in the water compartment [2].

In relation to metals, these can be deposited in sediments and also interact with other chemical species present and be effectively fixed in sediment in a non-bioavailable form. Furthermore, they can also be present in ways that can be accessible to local biota, as inorganic or organic complexes, or even in the soluble form (ionic) [2, 3].

However, when dealing with artificial reservoirs, this issue becomes complex, especially in function of their allochthonous characteristics. Artificial reservoirs have high sedimentation rates, when compared to those rivers that flow into them, which are lotic systems, while the reservoirs are lentic systems. The recent formation and well-documented history of most artificial reservoirs allows their paleolimnological records to be used in ways that are difficult in natural systems, for example in calibrating relative sedimentation rate with respect to the construction of the reservoirs and this contributes to separate

anthropogenic and geogenic processes along the sediment cores [4].

The clear difference between geogenic and anthropogenic concentrations is crucial for a correct environmental assessment. Often, the anthropogenic enrichment of a given element can cause concern. However, high concentrations do not necessarily mean toxic effects since metals can be immobilized in different forms in the environment either as sulfides, or complexed with organic matter. It is known that quality guideline values for sediments used internationally (for example; PEL, TEL, crustal averages) may not be suitable for tropical conditions which can lead to errors of interpretation in evaluations of metals in water bodies [5–10].

Several authors assessing metal availability in sediments have used sequential extraction to characterize the mobility and the bioavailability of metals in the sediment [11–17]. Associated phases may be different, depending on the reagents used and modifications employed by several authors, but generally include the following: exchangeable fraction; fraction bound to carbonates; fraction linked to reducible oxides; fraction associated with sulfides and total fraction [15–18].

Besides metals, another category of elements has shown an increase of interest, rare earth elements (REEs). Current applications of this group of elements have grown in the world and their use varies from laboratory tests to the doping of metallic alloy for strengthening of specific properties to agricultural uses. Relating to sequential extraction, there are few papers in the literature [19–25], related to their behavior to ligands in sediments and/or sedimentary profiles in different environments.

After all the considerations above, the objectives of the present study are: (a) to present a survey of some REEs distribution in a sedimentary profile at Jurumirim Reservoir using sequential extraction protocols; (b) to present total mass fractions for some REEs and other trace elements of environmental interest and (c) to assess if there is any anthropogenic influence on the concentrations of these elements in this reservoir. Furthermore, the data of this study can be used to develop a sediment REE mass fraction data bank in water supply reservoirs and to establish background values for REEs.

Experimental

Study area

The Jurumirim Reservoir is located in the southwestern region of the State of São Paulo, next to the Paraná State border. It is the first reservoir built on the Paranapanema River, its main river, and one of the main rivers of the Paraná Basin. Its construction began in the late 1950's, and its dam was completed in 1962, when electrical generation started. Its total drainage area is 17.8 thousand km^2 with a maximum volume of storage 6.5 $\times$ 10^9 m^3 and a flood area of 449 km^2.

This reservoir is located in the Paraná Basin almost entirely in the Serra Geral Formation (basic volcanic; Mesozoic), with a small portion of sedimentary rocks (Paleozoic) [26, 27].

The occupation of the watershed is characterized by the drainage area occupied by 14 % of preserved areas (forests and savannah). Only 2 % (about 800,000 inhabitants) of the population of the State is located in this river basin, considered the largest water resource management unit of the State of São Paulo in territorial extension with 22,689 km^2 [28].

Sampling and sample preparation

In January 2013, a sedimentary profile of 41 cm was collected in this reservoir. The collection was carried out with the aid of a boat with echo sounding, to locate the original bed of the Paranapanema River and carry out the collection of the profile on the original bed of the river. This profile was sliced at every 2.5 cm, totaling 16 fractions, packed in zip type bags and kept refrigerated until the time of sample preparation. Figure 1 shows the location of the sampling point with the coordinates S 23°14′ 364 and W 49°12′426.

In the laboratory, part of the samples were separated for grain-size determinations, another part was separated for chemical analysis and the rest was dried in a ventilated oven at 30–40 °C until constant weight and separated to total concentration and sequential extraction determinations.

Grain-size determination

Grain-size distribution was determined by laser scattering (Cilas 1090L particle analyser) at the Environmental Analysis Laboratory of the University of Campinas. The samples were dispersed by adding 40 mL of an aqueous solution of sodium hexametaphosphate (40 g L^{-1}) to 1.0 g of sediment and shaken for 24 h.

Sequential extraction protocol

For the sequential extraction of sediments, the extraction procedure suggested by the European Commission recommended and certified for BCR-701 reference material was employed [29]. The method is divided into three extractable phases plus the residual phase. The three steps were added together and then subtracted from the total content of the elements for obtaining the residual fraction,

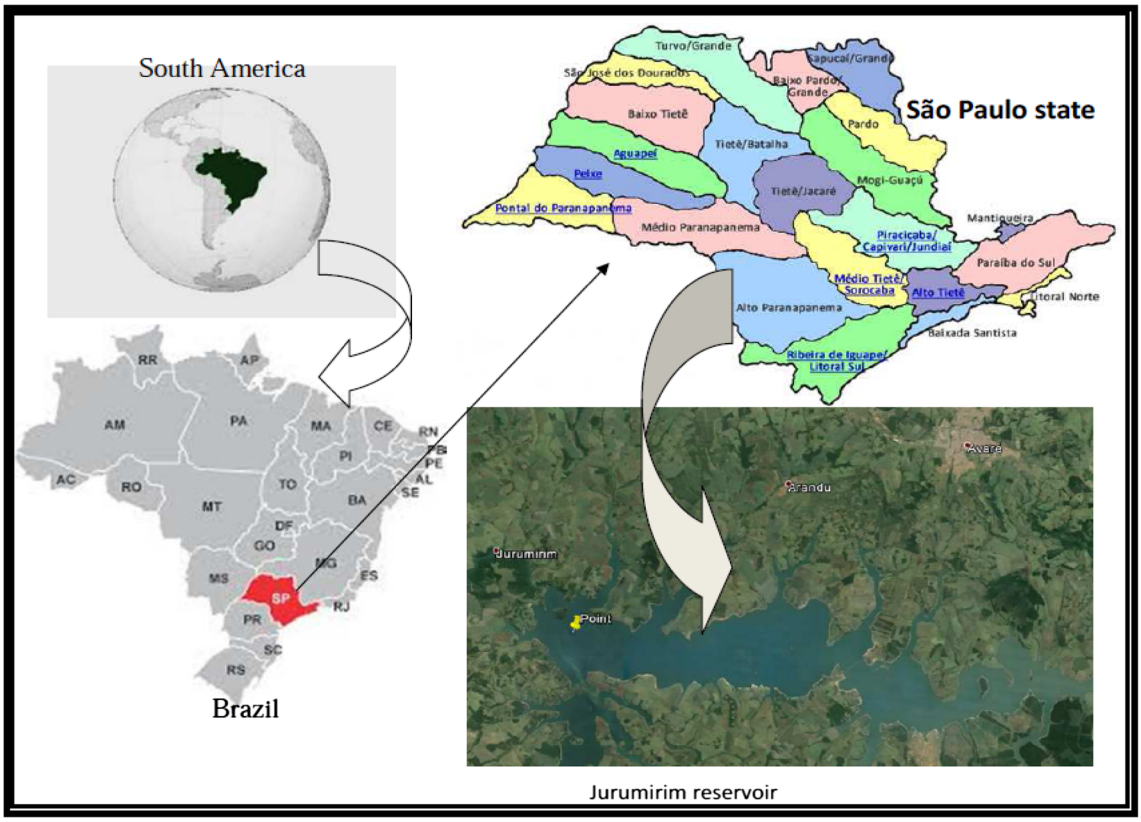

Fig. 1 Sampling point localization

the fourth step. Approximately 1 g of sediment (duplicate samples) and reference materials were weighed. The sequential extraction protocol was employed in the first nine fractions of the profile, corresponding to the depth of 22.5 cm.

To assess the efficiency of the extraction procedure, the BCR 701 reference material (certified in four phases for the elements Cd, Cu, Cr, Pb, Ni, and Zn) was extracted and measured under the same conditions. There is no certified reference material available for sequential extraction procedure for REEs.

The quantification of the metals Cr, Cu, Ni and Zn by ICP-OES (Inductively Coupled Plama Optical Emission Spectrometry) and Cd, Pb, Sc, Th, U and the REEs (Eu, Gd, La, Lu, Tb and Yb) by ICP-MS (inductively coupled plasma—mass spectrometry) in the steps of extracts were carried out. Some light (La), medium (Eu, Gd and Tb) and heavy (Yb and Lu) rare earths were selected to validate the analytical technique by ICP-MS. The uncertainties calculation in all chemical analysis were obtained according to Franklin et al. [30] and are presented for the results of the CRM analyses and ranged from 7 % for the element Cd and to 13 % for the element Gd. These analyses were performed at the Inorganic Chemistry Laboratory of the Environmental Agency of São Paulo State (CETESB). The analytical conditions of the element determinations for ICP-OES and ICP-MS are shown in Table 1.

Total mass fraction determined by ICP-MS and ICP-OES

Samples (in duplicate) were digested in a microwave oven similar to recommended by EPA 3052 method [31]. The digestion procedure was done by weighing about 0.4 g of samples in Teflon vials with the addition of 9 mL HNO_{3conc} + 4 mL HF_{conc} and digested in a microwave oven for 40 min, with maximum pressure of 200 psi. After this, a complementary step of digestion with 4 ml of boric acid (saturated solution) was added to neutralize the effects of fluoride precipitation of trivalent elements.

After digestion, samples were transferred to polyethylene tubes and appropriate dilutions were applied for quantification of the following elements: Cu, Ni and Zn by ICP-OES, and Cd, Pb and Gd by ICP-MS, according to conditions described in Table 1. For validation of both analytical methodologies (ICP-MS and ICP-OES) according to precision and accuracy, the reference materials San Joaquim Soil (SRM 2709a), Buffalo River Sediment (SRM 8704) and New Jersey Waterway Sediment (SRM 1944) from the National Institute of Standards and Technology

Table 1 Experimental conditions for analytical determinations for the elements by ICP-OES and ICP-MS

Element	Method	Line emission or mass	Detection limit (μg L^{-1})
Cu	ICP-OES	324.7 nm	0.2
Ni	ICP-OES	231.6 nm	0.2
Zn	ICP-OES	213.8 nm	1.0
Cr	ICP-OES/ICP-MS	267.7 and mass 52	1.0 and 0.05
Cd	ICP-MS	Mass 111	0.002
Pb	ICP-MS	Mass 206	0.01
Gd	ICP-MS	Mass 157	0.001
Eu	ICP-MS	Mass 153	0.001
La	ICP-MS	Mass 139	0.001
Lu	ICP-MS	Mass 175	0.0005
Tb	ICP-MS	Mass 159	0.001
Yb	ICP-MS	Mass 172	0.0005
Sc	ICP-MS	Mass 45	0.05
Th	ICP-MS	Mass 232	0.001
U	ICP-MS	Mass 238	0.0005

(NIST) were analysed. The uncertainties calculation in all chemical analyses were done according to Franklin et al. [30]. These analyses were performed in the Inorganic Chemistry Laboratory of the Environmental Agency of São Paulo State (CETESB).

Total mass fraction determined by instrumental neutron activation analysis (INAA)

For determination by INAA, approximately 150 mg of sediment (duplicate samples) and reference materials were accurately weighed and sealed in pre-cleaned double polyethylene bags, for irradiation. Sediment samples and reference materials were irradiated for 8 h under a thermal neutron flux of 10^{12} n cm^{-2} s^{-1} in the IEA-R1 nuclear research reactor at IPEN. Two series of countings were made: the first, after one-week decay and the second, after 15–20 days. Gamma spectrometry was performed using a Canberra HPGe detector and associated electronics, with a resolution of 0.88 and 1.90 keV for ^{57}Co and ^{60}Co, respectively. The elements determined by using this methodology were Cr, Sc, Th, U and the REEs (Ce, Eu, La, Lu, Nd, Sm, Tb, Yb). The analysis of the data was performed with in house software: VISPECT program to identify the gamma-ray peaks and by ESPECTRO program to calculate the concentrations. Sample and standard counting statistics and sample and standard masses were considered in the uncertainty assessment of the results. The counting statistics component is the most important contribution to activity uncertainty in INAA [32]. For methodology validation regarding precision and accuracy reference materials Soil 5 (IAEA), Lake Sediment SL1 (IAEA) and BEN Basalt-IWG-GIT were used.

Results and discussion

Grain-size distribution and sedimentation rate

Figure 2 presents the grain-size distribution of the sediment profile analysed.

The sedimentary profile collected proved to be quite homogeneous with respect to their granulometric distribution, with a ratio of 45–55 % of silt and 45–55 % of clay until slice 09 (20.0–22.5 cm). After this, the particle size composition presented some variations, with some slices presenting almost 10 % of sand in their composition. These particle size composition changes start at slice 10 (25.0–27.5 cm) and are evidence that the profile collected reached the sediment of the river before the construction of the reservoir, in 1960. From slice 01–09, the sediment corresponds to deposition from the existence of the reservoir, and below (10–16), the sediment corresponds to the Paranapanema River, where the reservoir was built.

Considering that the dam was built in 1960, and that the profile presents strong change in grain size distribution in the first 25 cm, the sedimentation rate of the Jurumirim Reservoir can be calculated as 25 cm over 55 years, resulting in a sedimentation rate of approximately 0.45 cm per year.

Extraction sequential protocol results

Table 2 shows the results obtained for the BCR 701 reference material analysis according to the Bureau of the European Community protocol for the certified elements.

Recovery for all elements analysed ranged from 70 to 120 %, which proved the efficiency of the protocol for the

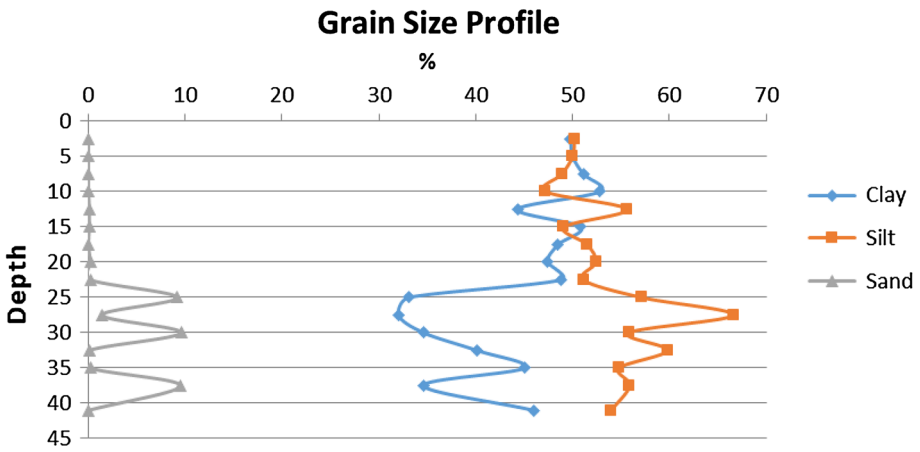

Fig. 2 Silt, clay and sand distribution in the sediment profile

Table 2 Element mass fractions in mg kg^{-1} (mean value and expanded uncertainties, k = 2), obtained for metals in the BCR 701 reference material analysis (BCR protocol) in comparison to certified values

	Step 1	Recovery (%)	Step 2	Recovery (%)	Step 3	Recovery (%)	Step 4	Recovery (%)
Cd								
Obtained	7.26 ± 0.49		2.9 ± 0.2		0.21 ± 0.03		0.15 ± 0.03	
Certified	7.3 ± 0.4	99.5	3.77 ± 0.28	77	0.27 ± 0.06	78	0.13 ± 0.08	115
Cr								
Obtained	3.44 ± 0.87		50.7 ± 3.2		156 ± 8		65 ± 4	
Certified	2.26 ± 0.16	152	45.7 ± 2.0	90	143 ± 7	109	63 ± 8	103
Cu								
Obtained	55.3 ± 3.4		130 ± 8		64.4 ± 5.8		35 ± 3	
Certified	49.3 ± 1.7	112	124 ± 3	108	55 ± 4	117	39 ± 12	90
Ni								
Obtained	18.5 ± 2.1		31.3 ± 2.9		16.3 ± 2.3		32 ± 3	
Certified	15.4 ± 0.9	120	26.6 ± 1.3	118	15.3 ± 0.9	107	41 ± 4	78
Pb								
Obtained	3.76 ± 0.43		149 ± 14		9.7 ± 0.8		12 ± 1	
Certified	3.18 ± 0.21	118	126 ± 3	118	9.3 ± 2.0	104	11 ± 6	109
Zn								
Obtained	216 ± 13		121 ± 9		44.1 ± 3.5		85 ± 5	
Certified	205 ± 6	105	114 ± 5	106	46 ± 4	96	95 ± 13	89

BCR 701 reference material analysis, except for Cr in step 1 that showed a recovery of 152 %.

The results obtained for metals are in accordance with the values of BCR protocol analysis certificates of the European Commission. The use of the CRM for validation of the method of sequential chemical extraction showed adequacy for the specific needs and ensured the quality of application of this procedure.

From the results obtained for the reference material analyses the protocol was applied to the sediment samples and the elements determined in the respective steps of the protocol [29]. The results are presented in Table 3.

Some elements presented higher concentrations in the residual phase especially for Cr, Ni, Sc, Th, and U, with concentration higher than 70 % at this step along the profile and very similar behavior between the slices. Thorium is present at about 95 % of its total concentration at this stage, and Sc remained at 80 % and about 15 % in the oxidizable fraction.

Still regarding the residual phase, the elements Cu and Zn also presented concentrations between 50 and 70 % along the profile. Cu also presented a relatively significant concentration in the oxidizable fraction (15–20 % over the profile). Zinc presented at about 10–15 % of its concentration in the phase associated with Fe–Mn oxides. Furthermore, in this reducible fraction, Pb concentration ranged from 44 to 71 % in relation to its total concentration and residual fraction being the second most important, with about 30 % of the total metal.

Table 3 Results (mg kg^{-1}) for trace and REEs in geochemical fractions (mg kg^{-1}) obtained by BCR sequential extraction protocol, total content and residual phase

Depth (cm)	Cd	Cr	Cu	Ni	Pb	Sc	Th	U	Zn	La	Eu	Gd	Tb	Yb	Lu
Exchangeable and acid soluble (fraction 1)															
2.5	0.038	0.44	4.62	2.48	0.21	0.61	0.019	0.18	5.69	2.58	0.12	0.68	0.11	0.21	0.033
5.0	0.040	0.45	5.27	2.61	0.24	0.70	0.025	0.19	5.96	3.28	0.13	0.87	0.14	0.26	0.040
7.5	0.036	0.45	4.51	1.86	0.23	0.68	0.019	0.16	4.75	2.37	0.12	0.81	0.11	0.20	0.031
10.0	0.037	0.54	5.00	2.39	0.25	0.76	0.024	0.19	5.61	3.21	0.13	0.98	0.14	0.26	0.040
12.5	0.042	0.48	4.90	2.26	0.34	0.77	0.028	0.20	6.41	3.37	0.16	0.85	0.14	0.27	0.042
15.0	0.048	0.59	4.94	2.13	0.34	0.76	0.025	0.17	6.96	3.37	0.16	1.16	0.14	0.27	0.043
17.5	0.042	0.37	4.83	1.79	0.30	0.80	0.023	0.15	5.82	3.02	0.14	1.02	0.13	0.26	0.040
20.0	0.044	0.53	5.09	2.31	0.28	0.75	0.026	0.16	7.16	4.06	0.18	1.25	0.17	0.32	0.050
22.5	0.041	0.32	5.18	2.11	0.28	0.79	0.021	0.14	6.52	3.28	0.15	0.91	0.14	0.28	0.044
Reducible (Oxy-hydroxides of Fe–Mn) (fraction 2)															
2.5	0.011	3.56	5.20	1.59	12.94	0.72	0.055	0.29	11.7	19.00	0.51	4.32	0.54	1.02	0.15
5.0	0.011	4.00	6.02	1.72	14.01	0.76	0.058	0.28	12.0	16.50	0.51	4.32	0.53	1.03	0.16
7.5	0.011	3.53	6.53	1.40	11.67	0.72	0.047	0.31	10.8	18.59	0.48	4.02	0.50	0.97	0.15
10.0	0.010	3.76	5.67	1.44	11.54	0.82	0.053	0.30	10.6	16.68	0.46	4.04	0.47	0.91	0.14
12.5	0.012	4.72	3.93	1.22	14.33	0.83	0.065	0.25	9.6	18.82	0.44	3.90	0.48	0.92	0.14
15.0	0.012	4.94	4.84	1.42	14.05	0.87	0.073	0.28	11.2	19.85	0.46	3.96	0.49	0.94	0.14
17.5	0.012	4.18	5.08	1.29	11.63	0.88	0.069	0.28	10.4	17.43	0.46	3.86	0.48	0.94	0.14
20.0	0.011	4.79	3.80	1.31	15.16	0.84	0.080	0.26	9.3	22.91	0.46	3.96	0.49	0.95	0.14
22.5	0.014	4.36	4.66	1.48	16.08	0.85	0.064	0.27	11.8	21.16	0.52	4.34	0.54	1.04	0.16
Oxidable (Organic matter and sulphides) (fraction 3)															
2.5	0.002	4.21	8.62	1.97	2.14	3.20	0.48	0.59	6.24	1.78	0.15	1.03	0.15	0.36	0.056
5.0	0.003	5.04	10.14	1.94	2.57	3.69	0.42	0.56	6.57	1.80	0.16	1.04	0.16	0.37	0.058
7.5	0.003	4.16	8.08	1.75	1.83	3.40	0.36	0.47	5.76	1.73	0.13	1.01	0.13	0.30	0.047
10.0	0.002	4.46	8.68	1.68	2.40	3.64	0.44	0.51	5.90	1.60	0.14	0.94	0.13	0.32	0.050
12.5	0.002	4.44	9.20	1.72	2.50	3.18	0.38	0.53	5.84	2.25	0.17	1.35	0.17	0.38	0.058
15.0	0.002	4.51	8.45	1.79	1.88	3.22	0.28	0.48	5.61	1.83	0.15	1.27	0.14	0.33	0.052
17.5	0.002	3.98	8.70	1.65	2.18	3.32	0.30	0.45	5.61	1.67	0.14	1.06	0.14	0.31	0.048
20.0	0.002	4.92	11.17	1.95	2.98	3.20	0.36	0.59	6.06	2.47	0.19	1.09	0.19	0.42	0.063
22.5	0.002	5.41	10.22	1.80	3.19	2.70	0.19	0.48	7.05	1.80	0.17	1.12	0.16	0.36	0.054
Sum of fractions 1, 2 and 3															
2.5	0.051	8.21	18.4	6.04	15.3	4.52	0.56	1.05	23.6	23.4	0.77	6.03	0.79	1.59	0.24
5.0	0.054	9.49	21.4	6.26	16.8	5.14	0.51	1.03	24.5	21.6	0.81	6.23	0.83	1.66	0.25
7.5	0.050	8.14	19.1	5.00	13.7	4.80	0.42	0.94	21.3	22.7	0.73	5.84	0.74	1.47	0.23
10.0	0.049	8.76	19.3	5.50	14.2	5.22	0.52	1.00	22.1	21.5	0.73	5.71	0.74	1.49	0.23
12.5	0.057	9.64	18.0	5.20	17.2	4.78	0.48	0.97	21.8	24.4	0.77	6.10	0.79	1.57	0.24
15.0	0.062	10.04	18.2	5.34	16.3	4.85	0.37	0.93	23.8	25.0	0.76	6.39	0.78	1.54	0.24
17.5	0.056	8.52	18.6	4.72	14.1	5.01	0.39	0.88	21.8	22.1	0.74	5.93	0.75	1.51	0.23
20.0	0.057	10.24	20.1	5.58	18.4	4.79	0.47	1.01	22.6	29.4	0.83	6.30	0.85	1.69	0.26
22.5	0.057	10.10	20.1	5.38	19.6	4.33	0.27	0.89	25.4	26.2	0.84	6.37	0.84	1.68	0.26
Residual (difference of total content—see Table 6—and sum of fractions)															
2.5	0.04	47.1	31.4	18.1	3.82	19.3	15.6	2.54	43.1	26.3	1.35	2.53	0.51	2.23	0.22
5.0	0.06	43.7	29.0	23.3	2.84	18.2	15.3	2.89	55.6	27.3	1.21	2.26	0.37	2.24	0.21
7.5	0.11	42.7	29.2	24.4	9.19	18.8	15.3	3.96	61.6	25.2	1.25	2.42	0.66	2.26	0.21
10.0	0.12	45.1	32.1	24.5	11.89	17.5	15.2	2.97	63.0	25.1	1.19	2.28	0.66	2.08	0.21
12.5	0.10	53.5	36.6	25.5	8.84	18.6	15.9	2.47	66.1	26.2	1.59	2.66	0.34	1.58	0.19
15.0	0.14	51.0	37.9	25.4	10.37	18.6	16.3	3.05	59.4	28.1	1.52	2.25	0.42	1.29	0.25
17.5	0.11	54.4	36.8	24.1	7.52	18.2	15.0	2.29	52.6	30.1	1.63	2.84	0.74	1.53	0.17

Table 3 continued

Depth (cm)	Cd	Cr	Cu	Ni	Pb	Sc	Th	U	Zn	La	Eu	Gd	Tb	Yb	Lu
20.0	0.11	50.5	34.6	24.5	7.19	18.4	16.2	3.00	61.2	22.4	1.43	2.48	0.69	1.31	0.17
22.5	0.13	48.2	39.6	23.4	6.63	18.8	15.1	3.19	53.3	25.1	1.36	1.58	0.57	1.39	0.23

Regarding the phase associated with the exchangeable cations and carbonates, Cd was the only element that presented significant concentration at this phase, with more than 25 % of its total concentration. It should be noted that Cd concentrations in the sequential extraction increase its partition between the residual phase versus soluble carbonate with the increase in depth. This may indicate a fixation of labile concentrations of this element in the sediment depth. The other elements did not present very significant concentrations at this fraction, presenting some concentrations exceeding 10 % in relation to the total.

For Cr, Cu, Ni, Zn, Cd, and Pb the sum of the fractions extracted (exchangeable and carbonate, Fe–Mn oxides, organic matter and sulfides) resulted in an average of 16, 36, 19, 30, 37 and 69 % of the total, respectively. The low concentrations of these elements in the more labile phases may indicate a lithological origin.

In the case of Pb, only 30 % of this element is present in the residual phase. According to some authors [17, 33, 34] it is not uncommon for Pb to bind with Fe–Mn oxides even in those environments that are not significantly impacted by human activities. This study area is located in a preserved region of São Paulo State. The most common behavior relative to the elements originated from anthropogenic activities can be associated with exchangeable phases, carbonates, organic matter and sulfides. [15–17, 33, 34] In the Jurumirim Reservoir, these labile phases were of little significance in relation to these elements.

The results for the REEs, in general, presented higher proportions in the residual phase, with about 60 % for Eu, 50 % for La and Yb, 45 % to Lu and 40 % to Tb. Gd, despite of presenting about 25–30 % of its concentration in the residual fraction, the fraction associated to oxides is more significant. For all other REEs evaluated, the residual phase was dominant, with the phase associated with Fe–Mn oxides always presenting lower concentrations.

Comparing the data of sequential extraction for the REEs in the Jurumirim Reservoir with other published studies in sediments, Leleyer et al. [20] noted that in the Piracicaba River, another important Brazilian river, the fractions associated to Fe oxides are in higher proportions and the residual fraction is the dominant fraction. The authors further mention that the dominant fractions may depend essentially on sediment constitution. The results obtained for the Jurumirim Reservoir were similar, with REEs presenting higher concentrations in the residual fraction, and the Fe–Mn oxide fraction being responsible for 35 % in average. These results were consistent with those results obtained for the Piracicaba River. In studies from other countries, the residual fraction and fraction associated to Fe–Mn oxides were also dominant.

Leybourne and Johannesson [35] analysing river sediments in Canada have determined that about 30 % of REEs are in the phase associated with Fe–Mn oxides. The values obtained for sediments from the Jurumirim Reservoir ranged from 20 to 45 %.

Liu et al. [21] analysing REEs by sequential extraction in sediments from Yellow River tributaries in China concluded that the residual fraction corresponded to more than 70 % of REEs, followed by oxidizable and carbonate associated fractions. Oxyhydroxide fraction was the less significant, accounting for merely 2 % of the REEs.

Song and Choy [23] in Chinese and Korean river sediment studies published that REEs are present in higher proportions in those fractions associated to the Fe oxides and residual phases and that grain-size and the source of the sediment have a significant impact in REEs behavior. Gd and Tb are present in significant concentrations in the reducible phase in the Jurumirim Reservoir.

Xu et al. [24] mentioned the same in studies of Bohay Bay in China, in a marine environment. The authors concluded that REEs are present in the residual fraction and the fraction associated to oxide and Fe–Mn oxyhydroxide have a significant importance in REE partition in sediments of the region, with the elements Eu, Gd and Tb having a slightly higher affinity for the Fe–Mn fraction in relation to other REEs.

Zhang et al. [19] in another study in the same location (Bohai Bay) concluded that REEs are more present in the residual phase, further mentioning that the granulometry influences this REE partition and are present in higher concentration in the residual phase when the sediment is coarse. In clayey sediments, the oxyhydroxide fraction has considerably more influence in the REE partition, yet with a dominant residual fraction. The same behavior was observed in the Jurumirim study.

In general, the sequential extraction in the Jurumirim Reservoir presented similar behavior, with little fluctuation in the concentration of the elements (including rare earth) along the profile. This suggests no significant changes in behavior of these elements over time, and recent anthropogenic contamination is thought to be of no importance in this reservoir.

Distribution of the elements along the sedimentary profile

Table 4 shows the results obtained for the CRM analyses by using EPA 3052 digestion procedure. Good recovery for all elements was obtained (from 88 %—Gd (SRM 2709a) to 101 %—Zn (SRM 8704)). The relative error ranged from 0 (Ni—SRM 1944) to 12.3 % (Gd—SRM 2709a) indicating good accuracy for the determination of these elements by ICP-OES and ICP-MS analytical techniques.

As can be seen in Table 5 the results for the three certified reference materials analyzed by INAA with relative standard deviation ranging from 1.4 to 14.3 % and relative error from 0 to 13.1 %, showed good precision and accuracy of the INAA technique, respectively.

Table 6 and Fig. 3a–c show the total elemental concentrations versus depth (cm) along the sediment profile from the Jurumirim Reservoir. The elements Cu, Ni and Zn were determined by ICP-OES; Cd, Pb and Gd, by ICP-MS and Cr, Sc, Th, U and REEs (La, Eu, Tb, Yb and Lu) by INAA.

In general, three element groups were separated according to their behavior along the sediment profile:

(a) Elements that presented a concentration increase from the bottom to the top: Cr, Sc, Th, and Yb;
(b) Elements with no or very small concentration fluctuations along the profile: Eu, Tb and Lu;
(c) Elements that showed some concentration fluctuations along the profile: Ni, Pb, U, and Zn.

Several elements presented a clear alteration in the concentration in the middle of the profile: Cr, Cu, Zn, Sc, Pb, and, Ni at the 25–30 cm depth. The granulometric composition of these two slices presented an increase in silt and sand proportions and a decrease in clay proportion, completely different from slices 5 to 20 cm deep, with a higher clay proportion. These changes are associated with the silt–clay proportion and was due to the profile having reached the sediment phase of the Paranapanema River before the flooding of the reservoir. This sediment core was collected in the Paranapanema bed with aid of an echo sounder.

These significant changes in the concentrations of the geogenic character elements is associated with the increase of the silty depth ratio with the presence of some sand, i.e. transitional phase of the sediment; reservoir phase, slices 1–9 (or 10), and after this, it is the river stage sediment.

However, the fluctuation of the concentrations of the elements along the profile suggests that elements varied according to silt–clay-sand ratio and its not clear behavior. This could suggest that the dam may not have suffered

Table 4 Element mass fractions in mg kg^{-1} (mean value and expanded uncertainties, $k = 2$), obtained in the reference material analyses by ICP-MS and ICP-OES

	SRM 1944			SRM 2709[a]			SRM 8704		
		R.E. (%)	Rec. (%)		R.E. (%)	Rec. (%)		R.E. (%)	Rec. (%)
Cu									
Obtained	359 ± 26	5.5	94.5	3179 ± 195	7.0	93.0			
Certified	380 ± 40			3420 ± 50					
Ni									
Obtained	74.2 ± 6.8	2.5	97.5	8.0 ± 0.9	0	100	40.5 ± 3.3	5.6	94.4
Certified	76.1 ± 5.6			8 ± 1			42.9 ± 3.7		
Zn									
Obtained	642 ± 29	2.1	97.9	4194 ± 120	0.3	100.3	412 ± 17	0.3	101
Certified	656 ± 75			4180 ± 20			408 ± 15		
Cd									
Obtained	8.5 ± 0.5	3.4	96.6				2.84 ± 0.21	3.4	96.6
Certified	8.8 ± 1.4						2.94 ± 0.29		
Gd									
Obtained				2.63 ± 0.25	12.3	87.7			
Certified				3.0 ± 0.1					
Pb									
Obtained	313 ± 26	5.2	94.8				134 ± 12	10.7	89.3
Certified	330 ± 48						150 ± 17		

RE relative error, *Rec* recovery

Table 5 Element mass fractions in mg kg^{-1} (mean value and expanded uncertainties, $k = 2$), obtained in the reference materials analysis by INAA ($n = 3$)

	Soil-5 (IAEA)				SL-1 (IAEA)				BE-N (Basalt IWG-GIT)			
	Certified value	Obtained value	RSD (%)	RE (%)	Certified value	Obtained value	RSD (%)	RE (%)	Certified value	Obtained value	RSD (%)	RE (%)
Cr	28.9 ± 2.9	28.2 ± 2.3	8.1	2.4	104 ± 9	107 ± 3	2.8	2.9	360 ± 12	368 ± 12	3.3	2.2
Sc	14.8 ± 0.66	14.8 ± 0.2	1.4	0	17.3 ± 1.1	15.8 ± 0.5	3.2	8.8	22 ± 1.5	22.0 ± 0.7	3.2	0
Th	11.3 ± 0.73	11.1 ± 0.5	4.5	1.8	14 ± 1	14 ± 1	7.1	0	10.4 ± 0.65	10.3 ± 0.5	4.8	0.4
U	3.04 ± 0.51	2.9 ± 0.2	6.9	4.6	4.02 ± 0.33	3.7 ± 0.2	5.4	8.0	2.4 ± 0.18	2.3 ± 0.3	13.0	4.2
Ce	59.7 ± 3.0	58.5 ± 3.2	5.5	2.0	105 ± 18	92 ± 5	5.4	9.5	152 ± 4	141 ± 18	12.8	7.2
Eu	1.18 ± 0.08	1.27 ± 0.05	3.9	7.6	1.6 ± 0.5	1.6 ± 0.1	6.3	0	3.6 ± 0.18	3.5 ± 0.2	5.7	2.8
La	28.1 ± 1.5	29.5 ± 1.5	5.1	5.0	52.6 ± 3.1	49.8 ± 3.6	7.2	5.3	82 ± 1.5	78 ± 9	11.5	4.9
Lu	0.336 ± 0.044	0.38 ± 0.03	7.9	13.1	0.54 ± 0.13	0.48 ± 0.04	8.3	11.1	0.24 ± 0.03	0.24 ± 0.02	8.3	0
Nd	29.9 ± 1.6	29.1 ± 1.7	5.8	2.7					67 ± 1.5	68 ± 6	8.8	1.5
Sm	5.42 ± 0.39	6.0 ± 0.3	5.0	10.7	9.25 ± 0.51	8.1 ± 0.2	2.5	12.4	12.2 ± 0.3	11.1 ± 1.4	12.6	9.0
Tb	0.665 ± 0.075	0.60 ± 0.05	8.3	9.8	1.4 ± 0.46	1.4 ± 0.2	14.3	0	1.3 ± 0.1	1.4 ± 0.2	14.3	7.7
Yb	2.24 ± 0.20	2.2 ± 0.2	9.1	1.8	3.42 ± 0.65	3.0 ± 0.1	3.3	12.3	1.8 ± 0.2	1.8 ± 0.1		

n number of determinations, *RSD* relative standard deviation; RE- relative error

Table 6 Total mass fraction (mg kg^{-1}) of the elements determined by ICP-MS, ICP-OES and NAA techniques

Depth(cm)	Cd**	Cr	Cu*	Ni*	Pb**	Sc	Th	U	Zn*	La	Eu	Gd**	Tb	Yb	Lu
2.5	0.089	55.3	49.8	24.2	19.1	23.8	16.1	3.6	66.8	49.7	2.13	9.56	1.3	3.8	0.47
5.0	0.115	53.2	50.4	29.6	19.7	23.3	15.8	3.9	80.1	48.9	2.01	9.74	1.2	3.9	0.47
7.5	0.156	50.9	48.4	29.4	22.9	23.6	15.7	4.9	82.9	47.9	1.99	9.25	1.4	3.7	0.44
10.0	0.164	53.9	51.4	30.0	26.1	22.8	15.7	4.0	85.1	46.6	1.92	9.43	1.4	3.6	0.44
12.5	0.156	63.1	54.7	30.7	26.0	23.4	16.4	3.4	87.9	50.6	2.36	9.87	1.1	3.2	0.43
15.0	0.199	61.1	56.2	30.8	26.6	23.5	16.7	4.0	83.2	53.1	2.29	9.84	1.2	2.8	0.49
17.5	0.163	62.9	55.4	28.8	21.6	23.2	15.4	3.2	74.4	52.2	2.38	9.41	1.5	3.0	0.40
20.0	0.163	60.7	54.7	30.0	25.6	23.2	16.6	4.0	83.8	51.9	2.26	9.48	1.5	3.0	0.43
22.5	0.188	58.3	59.7	28.8	26.2	23.2	15.4	4.1	78.7	51.4	2.20	9.34	1.4	3.1	0.48
25.0	0.192	47.4	61.3	31.4	25.9	24.5	13.0	2.2	83.7	49.1	2.10	8.97	1.0	2.8	0.41
27.5	0.102	50.2	34.6	18.1	17.4	24.3	13.7	2.6	54.8	48.9	1.97	9.22	1.1	2.9	0.42
30.0	0.212	45.0	66.4	29.5	25.6	19.0	12.1	2.5	78.9	46.8	1.89	9.65	1.4	3.0	0.40
32.5	0.205	54.1	55.2	27.5	23.9	27.1	14.1	2.5	80.8	53.2	2.20	9.75	1.4	3.2	0.49
35.0	0.233	45.9	49.5	23.9	32.9	22.8	13.3	3.3	65.2	49.3	2.45	9.50	1.2	2.9	0.48
38.0	0.142	37.6	39.3	20.7	17.7	17.9	11.1	2.6	65.4	44.6	2.08	9.68	1.1	2.7	0.42
41.0	0.171	39.0	38.3	23.0	20.1	14.9	10.2	2.6	68.5	41.6	1.73	9.58	0.9	2.6	0.41

* *Cu, Ni and Zn* determined by ICP-OES, ** *Cd, Pb and Gd* ICP-MS; others by INAA

significant changes in the deposition patterns of these elements. After dam construction, the concentration of the elements was stabilized, and before showed variations probably due to fluvial dynamics.

The rare earths Eu, Gd, La, Lu, and Tb showed a very similar distribution pattern in the sediment appearing not to be influenced by the granulometric differences along the profile. Only Yb showed an increase in concentration along the sediment profile.

Multivariate statistical analysis

Cluster analysis was performed using Ward's method and Euclidian distances (Fig. 4) with the data of total concentration for the elements determined by ICP-MS and ICP-OES (Table 6) and granulometric composition of the sediment samples along the profile. The purpose of this analysis was to verify similarities between elements (4a) and core samples (4b).

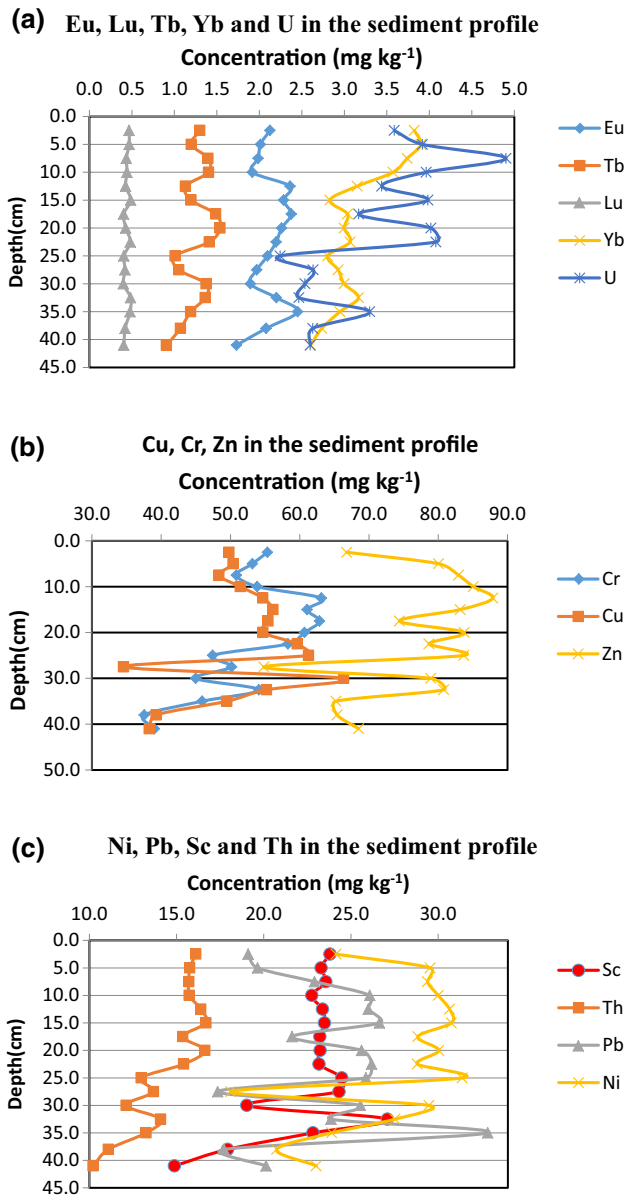

Fig. 3 **a–c** Elemental mass fraction × depth (cm) along the sediment profile from Jurumirim Reservoir

Two groups were identified:
Group 1, formed by 2 sub-groups:

- Sub-group A: samples 11, 15 and 16, separated by sand and silt;
- Sub-group B: samples 10, 12, separated by Pb, Cd, Zn, Ni and Cu;

Group 2, formed by 2 sub-groups:

- Sub-group A: samples 5, 6, 7, 8, 9, 13 and 14 grouped by Lu, Gd, Eu, Sc and La;
- Sub-group B: samples 1, 2, 3 and 4 grouped by Yb, Tb, Th, Cr and clay.

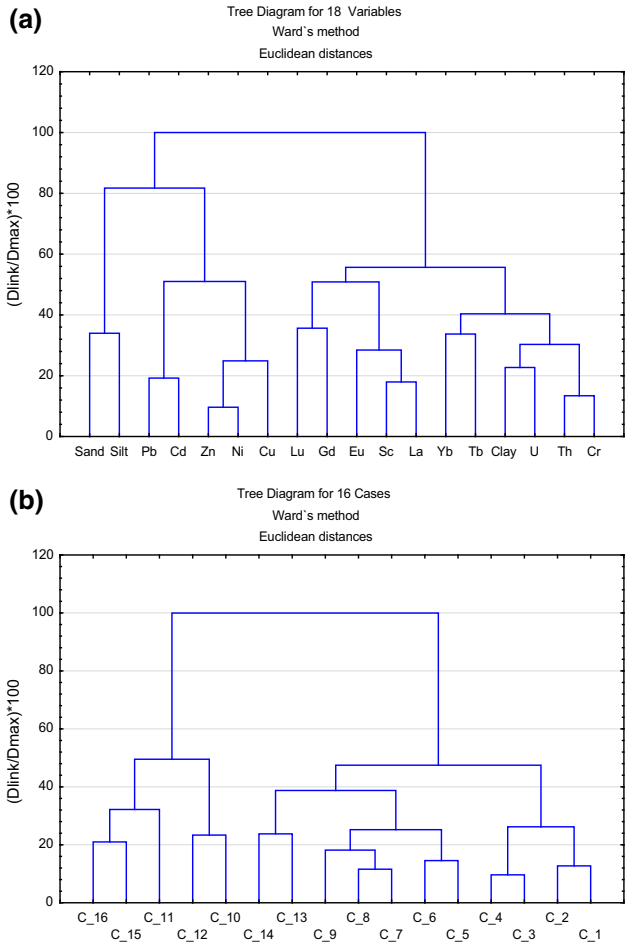

Fig. 4 Cluster analysis for the total mass fraction for the elements analysed by ICP-MS, ICP-OES, INAA and granulometric composition; **a** elements, **b** samples

The separation by elements (Fig. 4a) evidenced the behavior of the REE and elements that can be associated to them, such as Sc, U and Th; showed independent behavior of the clay fraction. The elements Pb, Cd, Zn, Ni and Cu, all bivalents, are more often associated with clay fractions, especially when found in their lithologic concentrations, as in this reservoir and showed more stable concentrations on the reservoir sediment phase. Figure 4b, separates the slices of the profile in slices of the river phase and reservoir phase, except for the slices 13 and 14, which were separated but displaced to one side of the slices associated with the reservoir phase.

Total mass fraction determined by INAA

Table 7 shows the results obtained by INAA for the REEs (Ce, Eu, La, Lu, Nd, Sm, Tb, Yb), and mass fraction of total REEs (ΣREE), light REEs (ΣLREE), heavy REEs (ΣHREE).

Table 7 Results (mg kg^{-1}) for total mass fraction for REEs by INAA, mass fraction of total REEs (ΣREE), light REEs (ΣLREE) and heavy REEs (ΣHREE)

Slice	Sediment type	La	Ce	Nd	Sm	Eu	Tb	Yb	Lu	ΣREE	ΣLREE	ΣHREE	ΣLREE/ΣHREE
1	Clayey	49.7	123	35	6.8	2.13	1.3	3.8	0.47	222.1	214.4	4.3	50.0
2	Clayey	48.9	115	39	6.8	2.01	1.2	3.9	0.47	217.5	209.9	4.4	48.0
3	Clayey	47.9	117	46	9.1	1.99	1.4	3.7	0.44	228.3	220.7	4.2	52.9
4	Clayey	46.6	108	42	9.2	1.92	1.4	3.6	0.44	213.2	205.9	4.0	51.3
5	Clayey	50.6	128	43	6.5	2.36	1.1	3.2	0.43	236.0	228.9	3.6	64.0
6	Clayey	53.1	126	48	8.6	2.29	1.2	2.8	0.49	242.5	235.7	3.3	71.1
7	Clayey	52.2	126	53	9.6	2.38	1.5	3.0	0.40	248.8	241.5	3.4	70.2
8	Clayey	51.9	127	55	7.9	2.26	1.5	3.0	0.43	249.2	241.9	3.4	70.6
Mean		50.1	122	45.3	8.1	2.2	1.3	3.4	0.44	232.2	224.9	3.8	59.7
SD		2.3	7	6.8	1.3	0.2	0.1	0.4	0.03	14.0	14.2	0.4	10.2
CV(%)		4.5	6	15.1	15.5	8.3	11.1	12.5	6.14	6.0	6.3	11.3	17.0
9	Silt and clay	51.4	131	52	8.4	2.20	1.4	3.1	0.48	250.6	243.5	3.6	68.6
10	Silt and clay	49.1	129	47	9.4	2.10	1.0	2.8	0.41	240.5	234.2	3.2	72.9
11	Silt and clay	48.9	124	40	8.9	1.97	1.1	2.9	0.42	227.8	221.4	3.3	66.1
12	Silt and clay	46.8	113	48	9.0	1.89	1.4	3.0	0.40	223.8	217.2	3.4	63.9
13	Silt and clay	53.2	139	53	10.3	2.20	1.4	3.2	0.49	262.8	255.5	3.7	70.0
14	Silt and clay	49.3	118	53	9.2	2.45	1.2	2.9	0.48	236.7	229.7	3.4	67.0
15	Silt and clay	44.6	102	50	8.9	2.08	1.1	2.7	0.42	211.7	205.4	3.2	65.1
16	Silt and clay	41.6	93	45	5.7	1.73	0.9	2.6	0.41	190.6	184.9	3.0	61.5
Mean		48.1	119	48.4	8.7	2.1	1.2	2.9	0.44	230.6	224.0	3.3	66.9
SD		3.7	16	4.7	1.3	0.2	0.2	0.2	0.04	22.6	22.2	0.2	3.6
CV (%)		7.7	13	9.6	15.2	10.5	16.3	6.3	8.63	9.8	9.9	6.3	5.4

The mean REEs mass fractions are generally similar in clayey silt that in sand and silty sand sediments, indicating that REEs contents in sediments are not related to grain size. In this case, there is no or little difference in the mean concentration between the two types of sediments found in this sediment profile.

Distribution patterns of REEs in the sediment profile

To study the distribution patterns of REEs, chondrite-normalization is widely applied [36]. The contents of REEs in chondrite proposed by Haskin et al. [37] are often cited.

The signature or pattern of the REEs is usually described by normalizing the individual REE concentrations of a sample to those of the crustal abundance of the earth. An average REE composition of shale is used for this normalization [38, 39].

The normalization of REE concentrations with respect to a geological "reference" value is a useful tool to obtain a comparison among information of "contamination" sources [40]. The results obtained and the NASC reference levels were normalized in relation to chondrite values [41] as reference values (Fig. 5). An enrichment of the light REEs (LREE) (La to Sm) and for the middle REEs (MREE) (Eu and Tb), and the same pattern for Yb and Lu (heavy—HREE) just as in the NASC values, were observed. Samples JRU-01, 02, 06, 09, 13 and 14 presented an enrichment of HREE and the others a depletion in relation to NASC values. This shows that these sediments may be comparable to shale that, in turn is representative of crustal average values.

Conclusions

The use of the CRM for the validation of the sequential extraction procedure showed adequacy for the specific needs and ensured the quality of application of this procedure.

For all elements evaluated, including some REEs, the residual phase was dominant, followed by the phase associated with Fe–Mn oxides always presenting lower concentrations, with the exception of Gd and Pb, which showed the Fe–Mn oxides as the most important phase, with higher concentrations.

Cluster analysis for the elements analysed evidenced the behavior of the REE and elements that can be associated to

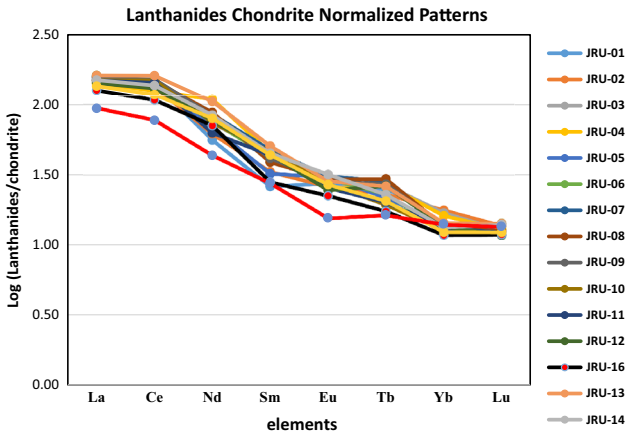

Fig. 5 Chondrite-normalized curves showing the distribution patterns of REEs in sediments

them, such as Sc, U and Th and showed independent behavior of the clay fraction. The elements Pb, Cd, Zn, Ni and Cu, all bivalents, are more often associated with clay fractions, especially when found in their lithologic concentrations, as in this reservoir. Cluster analysis for the samples, separates the slices of the profile in slices of the river phase and reservoir phase, except for slices 13 and 14, which were separated but displaced to one side of the slices associated with the reservoir phase.

The results of total content and the sequential extraction showed that the Jurumirim Reservoir seems not to have any recent anthropogenic contribution for the elements analysed. The results of this study can be used to establish not only a REE mass fraction data bank in this important water supply reservoir but also to establish REE background values for this region considered still preserved.

The distribution pattern of REEs according to Chondrite-normalization and NASC as reference values indicates that the sediments may be comparable to shale that, in turn is representative of crustal average values.

The construction of the dam appears to have not caused significant changes in the mass fraction of elements analysed in sediments from the river stage and the reservoir stage.

Acknowledgments The authors wish to thank professionals from Setor de Química Inorgânica and Setor de Amostragem from CETESB for their help and support in this study.

References

1. Esteves FA (1988) Fundamentos de Limnologia. Interciência/FINEP, Rio de Janeiro
2. CETESB (2011) Qualidade das Águas Superficiais do Estado De São Paulo 2010. CETESB, São Paulo
3. Chapman PM, Wang F, Germano JD, Batley G (2002) Pore water testing and analysis: the good, the bad and the ugly. Mar Poll Bull 44:359–366
4. Cohen AS (2003) Paleolimnology. The history and evolution of lakes systems. Oxford, New York
5. Audry S, Schaefer J, Blanc G, Jousnneau J-M (2004) Fifty-year sedimentary record of heavy-metal pollution (Cd, Zn, Cu, Pb) in Lot River Reservoirs (France). Environ Pollut 132:413–426
6. Gomes FC, Godoy JM, Godoy MLDP, Carvalho ZL, Lopes RT, Sanchez-Cabeza JAS, Lacerda LD, Wasserman JL (2009) Metal concentrations, fluxes, inventories and chronologies in sediments from Sepetiba and Ribeira Bays: a comparative study. Mar Poll Bull 59:123–133
7. Franklin RL, Fávaro DIT, Damatto SR (2016) Trace metal and rare earth elements in a sediment profile from the Rio Grande Reservoir, São Paulo, Brazil: determination of anthropogenic contamination, dating, and sedimentation rates. J Radioannal Nucl Chem 307(1):99–110
8. Vukovic Z, Vukovic D, Radenkovic M, Stankovic S (2012) A new approach to the analysis of the accumulation and enrichment of heavy metals in the Danube river sediment along the Iron Gate reservoir in Serbia. J Serb Chem Soc 77(3):381–392
9. Quináglia GA (2012) Caracterização de Níveis basais de concentração de Metais nos sedimentos do sistema estuarino da baixada Santista. Biblioteca24horas, São Paulo
10. Luiz-Silva W, Machado W, Matos RHR (2008) Multi-elemental contamination and historic record in sediments from the Santos-Cubatão estuarine system. Brazil J Braz Chem Soc 19(8):1490–1500
11. Sutherland RA (2000) Bed sediment-associated trace metals in an urban stream, Oahu, Hawaii. Environ Geol 39(6):611–627
12. Donahoe RJ, Liu C (1998) Pore water geochemistry near the sediment-water interface of a zoned, freshwater wetland in the southeastern United States. Environ Geol 33(2/3):143–153
13. Munk L, Faure G (2004) Effects of pH fluctuations on potentially toxic metals in the water and sediment of the Dillon Reservoir, Summit County. Colorado Appl Geochem 19:1065–1074
14. Wiechula D, Loska K, Korus I (2005) Lead partitioning in the bottom sediment of Rybnik reservoir (Southern Poland). Water Air Soil Pollut 164:315–327
15. Pereira JC, Silva AKG, Nalini HA Jr, Silva EP, Lena JC (2007) Distribuição, fracionamento e mobilidade de elementos traço em sedimentos superficiais. Quím Nova 30(5):1249–1255
16. Bevilacqua JE, Silva IS, Lichtig J, Masini JC (2009) Extração seletiva de metais pesados em sedimentos de fundo do rio Tietê, São Paulo. Quím Nova 32(1):26–33
17. Korfali SI, Jurdi MS (2011) Speciation of metals in bed sediment and water of Qaraaoun Reservoir, Lebanon. Environ Monit Assess 178:563–579
18. Gleyzes C, Tellier S, Astruc M (2002) Fractionation studies of trace elements in contaminated soils and sediments: a review of sequential extraction procedures. Trends Anal Chem 21(8):451–467
19. Zhang Y, Gao X, Chen-Tung AC (2014) Rare earth elements in intertidal sediments of Bohai Bay, China: concentration, fractionation and the influence of sediment texture. Ecotoxicol Environ Saf 105:72–79
20. Leleyler L, Probst JL, Rouault R, Samuel J, Depetris P, Haida S, Mortatti J (1999) Distribution des terres rares dans les sédiments fluviaux: fractionnement entre les phases labiles et résiduelles. Earth Plan Sci 329:45–52
21. Liu JJ, Lai ZJ, Liu Y (2013) Study on speciation and fractionation of rare earth elements in surface sediments in Gansu, Ningxia and Inner Mongolia Sections of Yellow River. Spectrosc Spectr Anal 33(3):798–803
22. Martins VA, Dias JA, Laut LM (2013) Especiation of rare earth elements in surface sediments of Lagoon of Aveiro (N Portugal). J Coastal Res Spec Edn 65:64–69

23. Song YH, Choi MS (2009) REE geochemistry of fine-grained sediments from major rivers around the Yellow Sea. Chem Geol 266:328–342
24. Xu Y, Song J, Duan L, Li X, Yuan H, Li N, Zhang P, Zhang Y, Xu S, Zhang M, Yin X (2012) Fraction characteristics of rare earth elements in the surface sediment of Bohai Bay, North China. Environ Monit Assess 184:7275–7292
25. Willis SS, Johannesson KH (2011) Controls on the geochemistry of rare earth elements in sediments and groundwaters of the Aquia aquifer, Maryland, USA. Chem Geol 285:32–49
26. Mapa da Geologia do Brasil (2010) IBGE—Instituto Brasileiro de Geografia e Estatística. http://www.infoescola.com/mapas/mapa-da-geologia-do-brasil/, Accessed in 08 Nov 2014
27. Mapa Geológico do Estado de São Paulo (2006) CPRM—Serviço Geológico do Brasil. http://geobank.sa.cprm.gov.br/, Accessed in 08 Nov 2014
28. CETESB (2009) Relatório de Qualidade das Águas Interiores do Estado de São Paulo 2008. CETESB, São Paulo
29. Rauret G, Lopes-Sánchez JF, Luck D, Muntau H, Quavauviller P (2001) The certification of the extractable contents (mass fractions) of Cd, Cr, Cu, Ni, Pb and Zn in freshwater sediment following a sequential extraction procedure BCR 701. Eur Com https://ec.europa.eu/jrc/sites/default/files/rm/BCR-701_report.pdf, Accessed on 08 Nov 2014
30. Franklin RL, Bevilacqua JE, Fávaro DIT (2012) Organic and total mercury determination in sediments by cold vapor atomic absorption spectrometry: methodology validation and uncertainty measurements. Quim Nova 35(1):45–50
31. US-EPA (2015) Method 3052—microwave assisted acid digestion of siliceous and organically based matrices. http://www.epa.gov/waste/hazard/testmethods/sw846/pdfs/3052.pdf, Accessed on 10 Jan 2015
32. Moreira EG, Vasconcellos MBA, Saiki M (2006) Uncertainty assessment in instrumental neutron activation analysis of biological materials. J Radioanal Nucl Chem 269(2):377–382
33. Lee PK, Jo HY, Chi SJ, Park SW (2013) Metal contamination and solid phase partitioning of metals in the stream and bottom sediments in a reservoir receiving mine drainage. Appl Geochem 28:80–90
34. Arain MB, Kazi TG, Jamali MK, Baig JA, Afridi HI, Jalbani N, Sarfrz RA (2009) Comparison of different extraction approaches for heavy metal partitioning in sediment samples. Pedosphere 19(4):476–485
35. Leybourne MI, Johannesson KH (2008) Rare earth elements (REE) and yttrium in stream waters, stream sediments, and Fe–Mn oxyhydroxides: fractionation, speciation, and controls over REE + Y patterns in the surface environment. Geochim Cosmochim Acta 72:5962–5983
36. Olmez I, Sholkovitz ER, Hermann D, Eganhouse RP (1991) Rare earth elements in sediments of Southern California: a new anthropogenic indicator. Environ Sci Technol 25:310–316
37. Haskin LA, Haskin MA, Frey FA, Wildeman TR (1968) Relative and absolute terrestrial abundances of the rare earths. In: Ahrens LH (ed) Origin and distribution of the elements. Pergamon Press, Oxford, pp 889–912
38. Taylor SR, Mc Lennan SM (1985) The continental crust: its composition and evolution. Blackwell Scientific, Palo Alto, pp 25–27
39. Henderson P (1984) In: Henderson P (ed) Rare earth element geochemistry. Elsevier, Amsterdam, p 1–32
40. Figueiredo AMG, Camargo SP, Sígolo JB (2009) Determination of REE in Urban Park Soils from São Paulo City for Fingerprint of Traffic Emission Contamination. In: Proceedings of the international Atlantic nuclear conference (INAC), Rio de Janeiro, September 26–October 02, Cd Rom
41. Masuda A (1962) Regularities in variation of relative abundances of lanthanide elements and an attempt to analyse separation-index patterns of some minerals. J Earth Sci Nagoya Univ 10:173–187